# Supplementary Information for "Surface topographic impact of subglacial water beneath Mars' south polar ice cap"

Authors: N.S. Arnold, F.E.G. Butcher, S.J. Conway, C. Gallagher and M.R. Balme

*Additional Model Data and Results*

Additional input details and results for some model runs are shown in Supplementary Figures 1-2. Initial conditions for the transient runs (see Methods) are shown in Supplementary Figure 1. There is ~ 200 m of relief in the bed topography (Supplementary Fig. 1a) over the area containing the water bodies, which (with the surface elevation (Fig. 1b)), leads to around ~ 200 m of ice thickness variation (Supplementary Fig. 1b). The effect of the LAPS in the NW corner is clearly seen in the thickness distribution; the bed topography here is fairly flat. The calculated steady-state flow velocity (Supplementary Fig. 1c) over the central area shows little spatial variation, with a mean annual velocity of ~ 2 x $10^{-7}$ $myr^{-1}$. The steep slopes over the LAPS lead to the largest velocities in the model domain, around $10^{-4}$ $myr^{-1}$. The calculated steady-state basal temperature largely reflects the ice thickness distribution. Over the central area (red box in Fig. 1b), basal temperatures vary by ~ 2K, with a mean value around 178K. This is very similar to the value calculated by Sori and Bramson[9]. The effect of the thinner ice beneath the LAPS is clearly seen, with basal temperatures of around 175K. The flow-induced elevation changes (Supplementary Fig. 1e) are very small over the central area, around $10^{-5}$ m over the 1000 year run duration, although they reach ~ +/- 0.2 m in the area at the crests of the LAPS due to the steep slopes and much faster resulting ice flow in this area. These values result in an annual synthesised mass balance of ~ $10^{-8}$ $myr^{-1}$ in the central part of the model domain (Supplementary Fig. 1f).

Supplementary Figure 2 shows additional results for Runs M1 and S9 (shown in Fig. 2a and b). The modelled ice velocity after 500 kyr (Supplementary Fig. 2a, Run M1) and 1 Myr (Supplementary Fig. 2b, Run S9) shows the enhancement due to sliding and softening of the ice due to geothermal heating. Velocity over the water bodies increases by a factor of ~ 600 (compared with the steady state velocity, Supplementary Fig. 1c) for Run M1, and by a factor of ~ 50 for Run S9. Thermally-driven softening increases the velocity over a larger area than sliding, but generally by a lower amount; by factors of ~ 100 and ~ 10 for Runs M1 and S9 respectively. Calculated basal temperatures for Runs M1 and S9

are shown in Supplementary Figs. 2c and d. For 90mWm$^{-2}$ (Run M1, Supplementary Fig. 2c), the basal temperature over the heated area increases to a mean of around 217K. This is approximately 15K higher than the values calculated by Sori and Bramson[9]. This could be partly due the simpler conductivity structure used in this study with uniform conductivity within the SPLD, although the steady state temperature (Supplementary Fig. 1c) suggests this is not an important effect. Instead, the higher calculated temperatures with high excess geothermal heat result from the strain heating feedback generated by the enhanced ice flow which forms an important additional source of basal heating, as argued by Butcher et al.[10] The calculated mean basal temperature for a geothermal heat flux of 60 mWm$^{-2}$ (Run S9, Supplementary Fig. 2d) is around 198K over the heated area. This is only slightly lower than the value for 72 mWm$^{-2}$ from Sori and Bramson[9], again showing the important additional heating component due to strain heating from enhanced flow.

Runs C11 - C14 (not shown) show that decreasing (increasing) ice thermal conductivity raises (lowers) the modelled basal temperature by a few K, leading to a slight enhancement (reduction) in elevation changes, mimicking a small increase (decrease) in excess geothermal heating. Altering ice density (to that of pure ice) has a similar effect to higher thermal conductivity via a different mechanism; it reduces calculated gravitational driving stress, lowering ice velocity and slightly reducing strain-induced heating, mimicking a slightly smaller level of excess geothermal heat. Acting together, lower ice conductivity has a slightly larger effect.

Run NS5 (not shown), with no sliding permitted but elevated GHF of 72 mWm$^{-2}$, shows a ~ +/- 0.25 m elevation height change in 500 kyr, with the largest values at the edge of the heated area, (as can be seen in Fig. 2a). The height change is less than that observed for run S9, showing that allowing basal sliding leads to more rapid and larger elevation changes than geothermal heating alone. Run NS10 (not shown) showed no long-term evolution of the surface topography due to possible effects of the basal topography on ice flow alone after a 10 My integration.

We also performed a set of runs (not shown) where the final conditions of Run S9 formed the initial conditions, and in which the geothermal anomaly was removed and sliding was prevented (simulating the end of the possible geothermal event, and re-freezing of the bed). The re-freezing results in a very rapid decrease in basal velocity over the

immediate area that was previously allowed to slide. The geothermally-induced increase in basal temperature diffuses away rapidly, at an exponentially-decreasing rate. After 500 kyr, the basal temperature in the heated areas is ~2 K above the initial value (shown in Supplementary Fig. 1d), and is within 0.5 K of the initial temperature by 2.5 Myr. The elevation changes due to heating and sliding result in a very small change in driving stress such that the elevation changes decay, but extremely slowly due to the very slow modelled ice velocity. After 10 Myr, the elevation anomalies have been reduced by ~ +/- 5 x $10^{-3}$ m.

Supplementary Figures

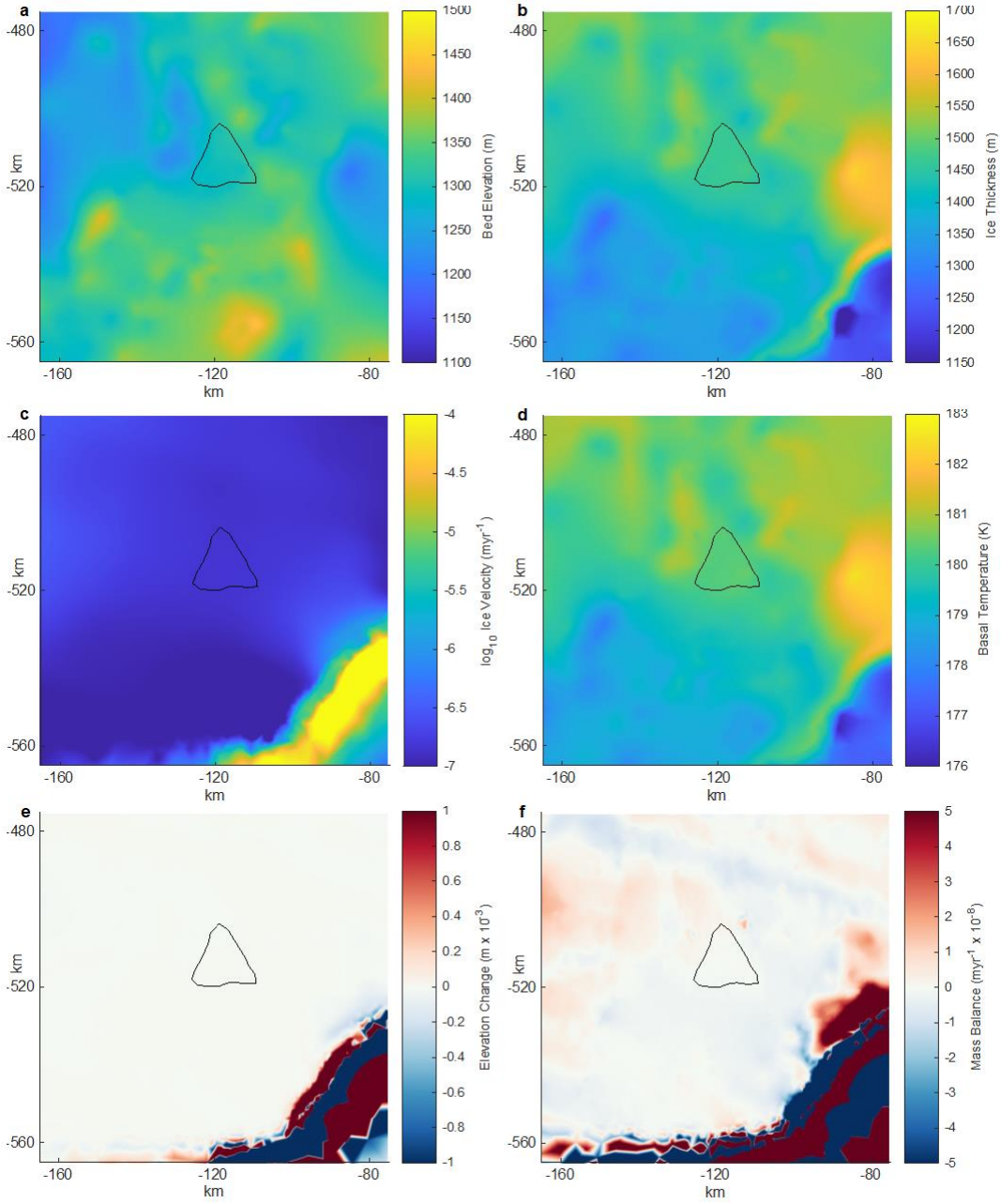


**Supplementary Figure 1. Boundary and initial conditions for the central area of the model domain (red square in Fig. 1b) for transient model runs**. **a**. MARSIS bed elevation[27]. **b**. MARSIS-derived SPLD thickness. **c**. Modelled steady state ice velocity (note logarithmic scale). **d**. Steady-state basal temperature. **e**. Modelled surface elevation change after 1000 model years without sliding or excess geothermal heating. **f**. Assumed surface mass balance from e. Outlines and axes as Fig. 1.

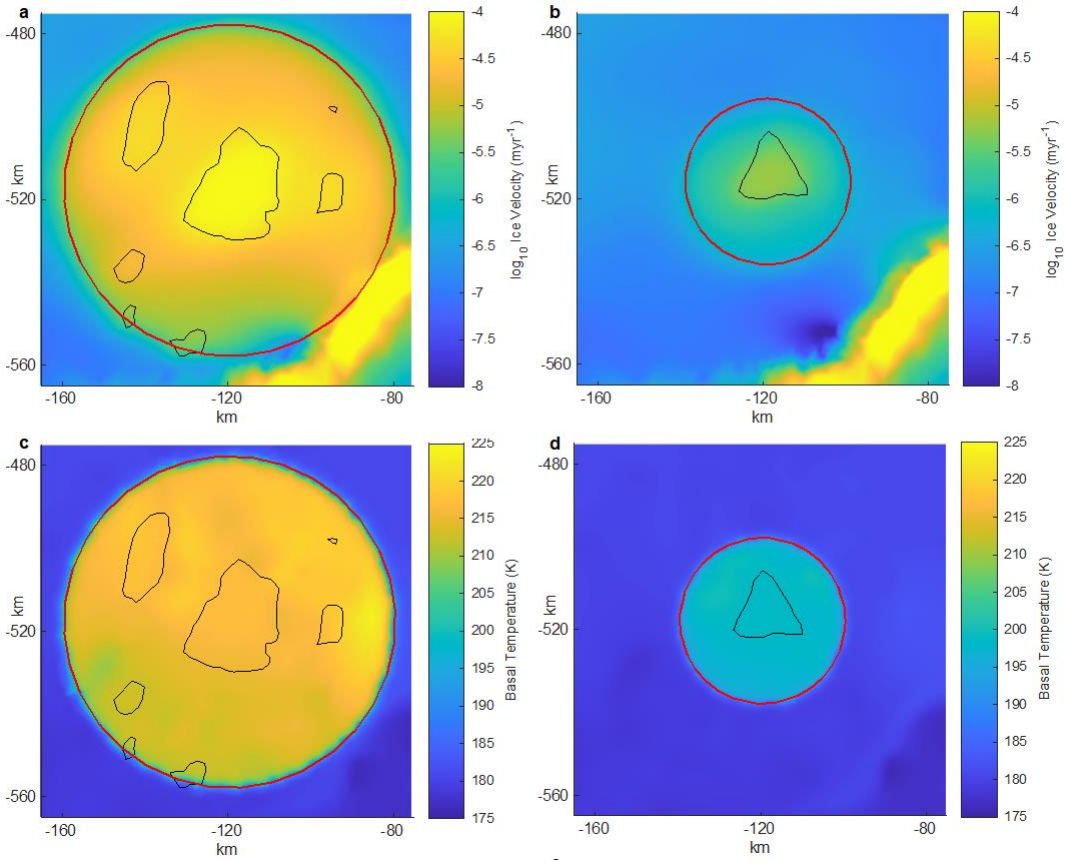


**Supplementary Figure 2. Additional model results for runs M1 and S9 for the central area of the model domain (red box in Fig. 1b) for transient model runs**. **a**. Modelled ice velocity for run M1 after 500 kyr. **b**. Modelled ice velocity for run S9 after 1 Myr. **c**. Modelled basal temperature for Run M1 after 500kyr. **d**. Modelled basal temperature for Run S9 after 1 Myr. Outlines and axes as Fig. 2.

Supplementary Tables

| Run | Elevated GHF ($mWm^{-2}$) | Radius of heating (km) | Sliding allowed | Parameters (Std denotes as Table S1) |
|---|---|---|---|---|
| M1 | 90 | 40 | M | Std |
| M2 | 72 | 40 | M | Std |
| M3 | 60 | 40 | M | Std |
| M4 | 90 | 30 | M | Std |
| M5 | 72 | 30 | M | Std |
| M6 | 60 | 30 | M | Std |
| M7 | 90 | 20 | M | Std |
| M8 | 72 | 20 | M | Std |
| M9 | 60 | 20 | M | Std |
| M10 | 30* | - | M | Std |
| S1-S10 | As M1-10 | As M1-10 | S | Std |
| C1-C10 | As M1-10 | As M1-10 | C | Std |
| L1-L10 | As M1-10 | As M1-10 | L | Std |
| LL6 | As M6 | 30** | L | Std |
| C11 | 60 | 30 | C | $\rho$ = 917 $kgm^{-3}$ |
| C12 | 60 | 30 | C | k = 2.0 $Wm^{-1}K^{-1}$ |
| C13 | 60 | 30 | C | k = 3.0 $Wm^{-1}K^{-1}$ |
| C14 | 60 | 30 | C | $\rho$ = 917 $kgm^{-3}$, k = 2.0 $Wm^{-1}K^{-1}$ |
| NS5 | 72 | 30 | No sliding | Std |
| NS10 | 30* | - | No sliding | Std |

**Supplementary Table 1. Model Runs**. M denotes sliding allowed over the multiple water bodies[2]. S denotes over the single central water body[1]. C denotes sliding over a circular water body in the location of the single water body of radius 12 km. L denotes over a lozenge-shaped area derived from the topographic bench identified here. 30** denotes an enlarged lozenge-shaped area equivalent to a 30km radius circle. * denotes nominal background geothermal heat for model domain[9].

| Parameter | Value | Source |
|---|---|---|
| SPLD Surface Temperature | 162 K | [9] |
| Background Geothermal Heat Flux | 30 $mWm^{-2}$ | [9] |
| Ice Density ($\rho$) | 1100 $kgm^{-3}$ | [2] |
| Ice Thermal Conductivity (k) | 2.4 $Wm^{-1}K^{-1}$ | [29] |
| *G* (Gravitational acceleration) | 3.711 $ms^{-2}$ | - |

**Supplementary Table 2. Standard Model Parameters**